A&A manuscript no.
(will be inserted by hand later)

Your thesaurus codes are:
02.04.01, 08.14.1, 08.16.6, 02.07.01

ASTRONOMY
AND
ASTROPHYSICS
1.2.2008

Radial pulsations and stability of protoneutron stars

D. Gondek, P. Haensel, and J.L. Zdunik

N. Copernicus Astronomical Center, Polish Academy of Sciences, Bartycka 18, PL-00-716 Warszawa, Poland
e-mail: dorota, haensel, jlz@camk.edu.pl

Abstract. Radial pulsations of newborn neutron stars (protoneutron stars) are studied for a range of internal temperatures and entropies per baryon predicted by the existing numerical simulations. Protoneutron star models are constructed using a realistic equation of state of hot dense matter, and under various assumptions concerning stellar interior (large trapped lepton number, zero trapped lepton number, isentropic, isothermal). Under prevailing conditions, linear oscillations of a protoneutron star can be treated as adiabatic, and evolutionary effects can be neglected on dynamic timescale. The dynamic behavior is governed by the adiabatic index, which in turn depends on the physical state of the stellar interior. The eigenfrequencies of the lowest radial modes of linear, adiabatic pulsations are calculated. Stability of protoneutron stars with respect to small radial perturbations is studied, and the validity of the static stability criteria is discussed.

Key words: dense matter – stars: neutron – stars: pulsars

1. Introduction

Newly born neutron stars are hot and lepton rich objects, quite different from ordinary low temperature, lepton poor neutron stars. In view of these differences, newly born neutron stars are called *protoneutron* stars; they transform into standard neutron stars on a timescale of the order of ten seconds, needed for the loss of a significant lepton number excess via emission of neutrinos trapped in dense, hot interior.

In view of the fact that the typical evolution timescale of a protoneutron star (seconds) is some three orders of magnitude longer, than the dynamical timescale for this objects (milliseconds), one can study its evolution in the quasistatic approximation (Burrows & Lattimer 1986). Static properties of protoneutron stars, under various assumptions concerning composition and equation of state (EOS) of hot, dense stellar interior were studied by numerous authors (Burrows & Lattimer 1986, Takatsuka 1995, Bombaci et al. 1995, Bombaci 1996, Prakash et al. 1997).

The scenario of transformation of a protoneutron star into a neutron star could be strongly influenced by a phase transition in the central region of the star. Brown and Bethe (1994) suggested a phase transition implied by the K^- condensation at supranuclear densities. Such a K^- condensation could dramatically soften the equation of state of dense matter, leading to a low maximum allowable mass of neutron stars. In such a case, the massive protoneutron stars could be stabilized by the effects of high temperature and of the presence of trapped neutrinos, and this would lead to maximum baryon mass of protoneutron stars larger by some 0.2 $M_\odot$ than that of cold neutron stars. The deleptonization and cooling of protoneutron stars of baryon mass exceeding the maximum allowable baryon mass for neutron stars, would then inevitably lead to their collapse into black holes. The dynamics of such a process was recently studied by Baumgarte et al. (1996). It should be mentioned, however, that the very possibility of existence of the kaon condensate (or other exotic phases of matter, such as the pion condensate, or the quark matter) at neutron star densities is far from being established. Recently, for instance, Pandharipande et al. (1995) pointed out, that kaon-nucleon and nucleon-nucleon correlations in dense matter raise significantly the threshold density for kaon condensation. In view of these uncertainties, we will restrict in the present paper to a standard model of dense matter, composed of nucleons and leptons.

The calculations of the static models of protoneutron stars should be considered as a first step in the studies of these objects. It is clear, in view of the dynamical scenario of their formation, that protoneutron stars are far from being static. The formation scenario involves compression (with overshoot of central density) and a hydrodynamical bounce, so that a newborn protoneutron star begins its life in a highly excited state, pulsating around its quasistatic equilibrium. If the rotation of protoneutron star is not too rapid, the coupling of radial and non-radial pulsations is weak. Such a scenario of formation leads to a preferential excitation of the radial modes. Having constructed

Send offprint requests to: D. Gondek

the static model of a protoneutron star, one should thus answer the question about the stability of the static configuration with respect to radial perturbations (standard stability criteria are valid only for cold neutron stars). Clearly, both high temperature and large trapped lepton number will influence the spectrum of radial eigenfrequencies of protoneutron stars, implying differences with respect to the case of cold neutron stars.

In the present paper we study the radial pulsations of protoneutron stars and their stability. Our models of protoneutron stars are composed of a hot, neutrino-opaque interior (hereafter referred to as "hot interior"), separated from much colder, neutrino-transparent envelope by a neutrinosphere. We will consider two limiting cases of the thermal state of the hot interior: isentropic, with entropy per baryon $s = const.$, and isothermal, with $T_\infty = (g_{00})^{1/2}T = const.$ (T_∞ is the value of the temperature, measured by an observer at infinity, while T is the value of the temperature measured by a local observer).

The first case, characteristic of a very initial state of a protoneutron star, will simultaneously correspond to a significant trapped lepton number. The second case corresponds to situation after the deleptonization of a protoneutron star. The position of the neutrinosphere will be located using a simple prescription based on specific properties of the neutrino opacity of hot dense matter. In all cases, the equation of state of hot dense matter will be determined using one of the realistic models of Lattimer and Swesty (1991).

The plan of the paper is as follows. In Section 2 we describe the physical state of the interior of protoneutron star, with particular emphasis on the EOS of the hot interior at various stages of evolution of a protoneutron star. We explain also our prescription for locating the neutrinosphere of a protoneutron star, and we give some details concerning the assumed temperature profile within protoneutron star. Equations of state, corresponding to different physical situations, are described in Section 3. We also present there static models of protoneutron stars, calculated for various assumptions concerning the hot stellar interior. In Section 4 we compare various timescales, characteristic of evolution and dynamics of a protoneutron star, which are essential for approximations used in the treatment of pulsations. Section 5 is devoted to the formulation of the problem of linear, adiabatic, radial pulsations of protoneutron stars. Both pulsations and stability involve the adiabatic index of pulsating stellar interior; our results for this important quantity are presented in Section 6. Numerical results for the eigenfrequencies of the lowest modes of radial pulsations and the problem of stability of protoneutron stars are presented in Section 7. Finally, Section 8 contains a discussion of our results and conclusion.

2. Physical model of the interior of protoneutron stars

We will consider a protoneutron star (PNS) just after its formation. We will assume it has a well defined neutrinosphere, which separates a hot, neutrino-opaque interior from colder, neutrino-transparent outer envelope. The parameters, which determine the local state of the matter in the hot interior are: baryon (nucleon) number density n, net electron fraction $Y_e = (n_{e^-} - n_{e^+})/n$, and the net electron-neutrino fraction $Y_\nu = Y_{\nu_e} - Y_{\bar{\nu}_e}$. The calculation of the composition of hot matter and of its EOS is described below.

2.1. Neutrino opaque core with nonzero trapped lepton number

The situation described in this subsection is characteristic of the very initial stage of existence of a PNS. Matter is assumed to be composed of nucleons (both free and bound in nuclei) and leptons (electrons and neutrinos; for the sake of simplicity, we do not include muons). All constituents of the matter (plus photons) are in thermodynamic equilibrium at given values of n, T and $Y_l = Y_e + Y_\nu$. The composition of the matter is calculated from the condition of beta equilibrium, combined with the condition of a fixed Y_l,

$$\begin{aligned} \mu_p + \mu_e &= \mu_n + \mu_{\nu_e} , \\ Y_l &= Y_e + Y_\nu , \end{aligned} \tag{1}$$

where $\mu_{\rm j}$ are the chemical potentials of matter constituents. At the very initial stage we expect $Y_l \simeq 0.4$. Electron neutrinos are degenerate, with $\mu_{\nu_e} \gg T$ (in what follows we measure T in energy units). The deleptonization, implying the decrease of Y_l, occurs due to diffusion of neutrinos outward (driven by the μ_{ν_e} gradient), on a timescale of seconds (Sawyer & Soni 1979, Bombaci et al. 1996). The diffusion of highly degenerate neutrinos from the central core is a dissipative process, resulting in a significant *heating* of the neutrino-opaque core (Burrows & Lattimer 1986).

2.2. Neutrino opaque core with $Y_\nu = 0$

This is the limiting case, reached after complete deleptonization. There is no trapped lepton number, so that $Y_l = Y_e$ and $Y_{\nu_e} = Y_{\bar{\nu}_e}$, and therefore $\mu_{\nu_e} = \mu_{\bar{\nu}_e} = 0$. Neutrinos trapped within the hot interior do not therefore influence the beta equilibrium of nucleons, electrons and positrons, and for given n and T the equilibrium value of Y_e is determined from

$$\mu_p + \mu_e = \mu_n , \tag{2}$$

while $\mu_{e^+} = -\mu_e$. In practice, this approximation can be used as soon as electron neutrinos become non-degenerate within the opaque core, $\mu_{\nu_e} < T$, which occurs after some ~ 10 seconds (Sawyer & Soni 1979, Prakash et al. 1997).

2.3. Neutrinosphere and the temperature profile

In principle, the temperature (or entropy per nucleon) profile within a PNS has to be determined via evolutionary calculation, starting from some initial state, and taking into account relevant transport processes in the PNS interior, as well as neutrino emission from PNS. Transport processes within neutrino-opaque interior occur on timescales of seconds, some three orders of magnitude longer than dynamical timescales. Convection can shorten neutrino transport timescale, but still the time needed for the deleptonization of the neutrino opaque core is then much longer than the dynamical timescale. The very outer layer of a PNS becomes rapidly transparent to neutrinos, deleptonizes, and cools on a very short timescale via e^-e^+ pair annihilation and plasmon decay to $T < 1$ MeV. It seemed thus natural to model the thermal structure of the PNS interior by a hot core limited by a neutrinosphere, and a much cooler, neutrino transparent outer envelope. The transition through the neutrinosphere is accompanied by a temperature drop, which takes place over some interval of density just above the "edge" of the hot neutrino-opaque core, situated at some n_ν.

In view of the uncertainties in the actual temperature profiles within the hot interior of PNS, we considered two extremal situations for $n > n_\nu$, corresponding to an isentropic and an isothermal hot interior. In the first case, hot interior was characterized by a constant entropy per baryon $s = const.$. In the case of trapped lepton number, this leads to the EOS of the type: pressure $P = P(n,\ [s, Y_l])$, energy density divided by c^2 (energy-mass density), $\rho = \rho(n,\ [s, Y_l])$, and temperature $T = T(n,\ [s, Y_l])$, with fixed s and Y_l. This EOS will be denoted by EOS$[s, Y_l]$.

The condition of isothermality, which in the static case corresponds to a vanishing heat flux, is more complicated. Due to the curvature of the space-time within PNS, the condition of isothermality (thermal equilibration) corresponds to the constancy of $T_\infty = (g_{00})^{1/2}T$ (see, e.g., Zeldovich & Novikov 1971, chapter 10.6). Actually, the isothermal state within the hot interior will be reached on a timescale corresponding to thermal equilibration, which is much longer than the lifetime of a PNS. Nevertheless, we considered the $T_\infty = const.$ models because, as a limiting case so different from the $s = const.$ one, it enables us to check the dependence of our results for PNS on the thermal state of the hot interior.

To determine the isothermal temperature profile in the hot interior after deleptonization, we use the condition of thermal equilibrium, given by the constancy of the function $T_\infty \equiv T(r)e^{\frac{1}{2}\nu(r)}$ (where $\nu(r)$ is the metric fuction, see Sect. 5). The relativistic condition of the isothermality can be rewritten as:

$$\frac{\mathrm{d}\ln T}{\mathrm{d}r} = \frac{1}{\rho c^2 + P}\frac{\mathrm{d}P}{\mathrm{d}r}\ . \tag{3}$$

This formula enables us to determine the $T(n)$ profile, for given EOS, *independently* of the specific structure of the stellar model under consideration.

Treating n, T as thermodynamic variables for our equation of state, we can rewrite Eq. (3) in the form:

$$\frac{\mathrm{d}\ln T}{\mathrm{d}\ln n} = \frac{P}{\rho c^2 + P} \times \left(\frac{\partial \ln P}{\partial \ln n}\right)\left\{1 - \frac{P}{\rho c^2 + P}\left(\frac{\partial \ln P}{\partial \ln T}\right)\right\}^{-1}\ . \tag{4}$$

Using the above formula we can construct a specific isothermal EOS, describing hot isothermal interiors, and parametrized by the boundary condition at the edge of the hot isothermal core - the value of T just below the neutrinosphere will be denoted by T_b. Thus in our relativistic calculations the set of the "isothermal" stellar configurations corresponds to stars with given T_b. Starting from $T = T_\mathrm{b}$, the temperature increases inward, reaching its maximum value in the center of the star where $T = T_\mathrm{centr}$. This central temperature is the function of the central density ρ_centr and is larger for a star with larger ρ_centr.

Our calculation of the neutrinosphere within the hot PNS interior is explained below. For a given static PNS model, the neutrinosphere radius, R_ν, has been located through the condition

$$\int_{R_\nu}^{R} \frac{1}{\lambda_\nu(E_\nu)}\mathrm{d}r_\mathrm{prop} = 1\ , \tag{5}$$

where λ_ν is calculated at the matter temperature, E_ν is the mean energy of non-degenerate neutrinos at and above the neutrinosphere, $E_\nu = 3.15T_\nu$, and r_prop is the proper distance from the star center. We assumed that neutrino opacity above R_ν is dominated by the elastic scattering off nuclei and nucleons, so that $\lambda_\nu = \lambda_\nu^0(n,T)/E_\nu^2$. Then, we determined the value of the density at the neutrinosphere, n_ν, for a given static PNS model, combining Eq. (5) with that of hydrostatic equilibrium, and readjusting accordingly the temperature profile within the outer layers of PNS.

Neutrino opacity in the outer layers of PNS can be well approximated by $1/\lambda_\nu \simeq \kappa_0 {E_\nu}^2$. Within a reasonable approximation $\kappa_0 \simeq \gamma\rho$, where ρ is the matter density, and $\gamma = 6 \cdot 10^{-20}$ cm^{-1} (ρ in g cm^{-3} and E_ν in MeV). The proper distance near the neutrinosphere is given by $\mathrm{d}r_\mathrm{prop} = (g_{rr})^{1/2}\mathrm{d}r \simeq (1 - 2GM/Rc^2)^{-1/2}\mathrm{d}r$. Using the definition of the neutrinosphere radius, R_ν, we can express the mass of the envelope above R_ν and the pressure at R_ν, denoted by P_ν, in terms of $E_\nu = 3.15T_\nu$. This leads to

$$P_\nu = 2.23\ 10^{32}\ \widetilde{M}\widetilde{R}^{-2}\left(1 - 0.295\frac{\widetilde{M}}{\widetilde{R}}\right)^{-\frac{1}{2}}\ {T_\nu}^{-2}\ \frac{\mathrm{erg}}{\mathrm{cm}^3}\ . \tag{6}$$

where $\widetilde{M} = M/M_\odot$ and $\widetilde{R} = R/10$ km.

For a given stellar model, this approximate relation, combined with Eq.(3), enables one to determine, in a self-consistent way, the values of T, n, and ρ at the neutrinosphere. In practice, this was done assuming a specific functional form of the temperature drop within the neutrinosphere (a combination of Fermi functions), which yielded a smooth transition between hot interior and cool envelope. In all cases, the temperature profile was adjusted in such a way, that neutrinosphere was found within the region of the temperature drop. For a 1.4 $M_\odot$ PNS, and an isothermal hot core with $T_\mathrm{b} = 15$ MeV, we found $T_\nu = 4.3$ MeV, $n_\nu = 2.0\ 10^{-3}$ fm^{-3}, and $\rho_\nu = 3.5\ 10^{12}$ g cm^{-3}. In the case of a very massive PNS with $M = 2\ M_\odot$ we obtained (for the same value of T_b) $T_\nu = 5.2$ MeV, $n_\nu = 2.4\ 10^{-3}$ fm^{-3}, and $\rho_\nu = 4.1\ 10^{12}$ g cm^{-3}. These results are in a reasonable agreement with those obtained in detailed numerical simulations (see, e.g., Burrows & Lattimer 1986).

3. Equation of state and static models of protoneutron stars

The starting point for the construction of our EOS for the PNS models was the model of hot dense matter of Lattimer and Swesty (1991), hereafter referred to as LS. Actually, we used one specific LS model, corresponding to the incompressibility modulus at the saturation density of symmetric nuclear matter $K = 220$ MeV (this model will be hereafter referred to as LS-220). For $n > n_\nu$ we supplemented the LS-220 model with contributions resulting from the presence of trapped neutrinos of three flavours (electronic, muonic and tauonic) and of the corresponding antineutrinos.

In Figs. 1-3 we show our EOS in several cases, corresponding to various physical condition in the hot, neutrino-opaque interior of PNS. For the sake of comparison, we have also shown the EOS for cold catalyzed matter, used for the calculation of the (cold) NS models. In Fig. 1 we show our EOS at subnuclear densities. At such densities, both the temperature and the presence of trapped neutrinos lead to a significant increase of pressure, as compared to the cold catalyzed matter. The constant T_∞ EOS stiffens considerably at lower densities, which is due to the weak dependence of the thermal contribution (photons, neutrinos) on the baryon density of the matter. It is quite obvious, that $T_\infty = const.$ EOS becomes dominated by thermal effects for $n < 10^{-2}$ fm^{-3}. On the contrary, for the isentropic EOS, the effect of the trapped lepton number ($Y_l = 0.4$) turns out to be more important than the thermal effects. This can be seen in Fig. 1, by comparing long-dashed curve, [$s = 2$, $Y_l = 0.4$], with a short-dashed line, which corresponds to an artificial (unphysical) case with small thermal effects, [$s = 0.5$, $Y_l = 0.4$].

It is clear, that the correct location of the neutrinosphere, which separates hot interior from the colder outer envelope, should be important for the determination of the radius of PNS.

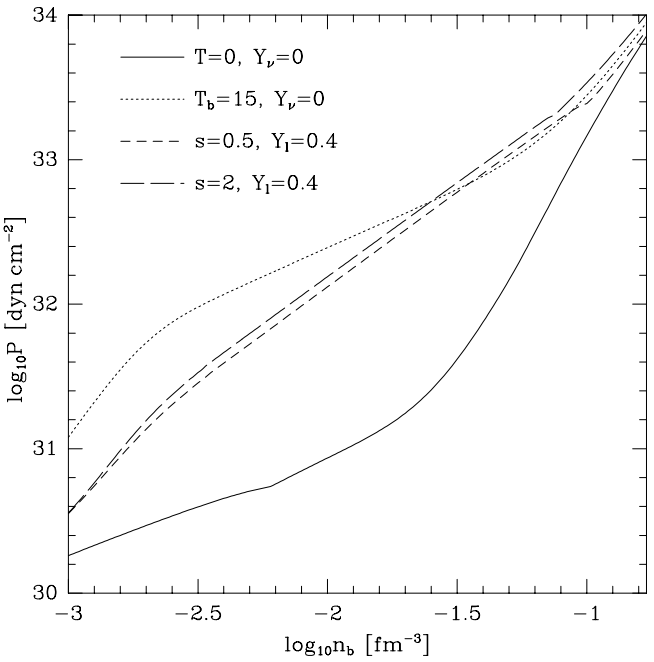

Fig. 1. Pressure versus baryon density for our model of dense hot matter (based on the LS-220 model of the nucleon component of the matter), under various physical conditions, for the subnuclear densities $n < n_0 = 0.16$ fm^{-3}. The curve $T = 0$ corresponds to cold catalyzed matter. The curve corresponding to $s = 0.5, Y_l = 0.4$ is unphysical, but has been added in order to visualize the importance of trapped lepton number at subnuclear densities. The low density edge of the hot, neutrino opaque core corresponds to $n_\nu = 2 \times 10^{-3}$ fm^{-3}.

Our EOS above nuclear density is plotted in Fig. 2. The presence of a trapped lepton number softens the EOS, while thermal effects always lead to pressure increase with respect to that for cold catalyzed matter. The softening of the supranuclear EOS at fixed Y_l is due to the fact, that a significant trapped lepton number increases the proton fraction, which implies the softening of the nucleon contribution to the EOS. This is the reason why pressure for [$s = 0.5$, $Y_l = 0.4$] model is smaller than in the case of cold, catalyzed matter.

In the calculations of the stellar structure the relevant EOS is of the form $P = P(\rho)$, because only pressure and mass–energy density appear in the general relativistic equations of hydrostatic equilibrium. It is obvious that thermal contribution to ρ is always positive. Also, the contribution of trapped neutrinos (which do not contribute to baryon number density n) to ρ is positive. However, large trapped lepton number implies an increased proton fraction, which in turn implies a *softening* of the nucleon contribution to the pressure. The interplay of these effects

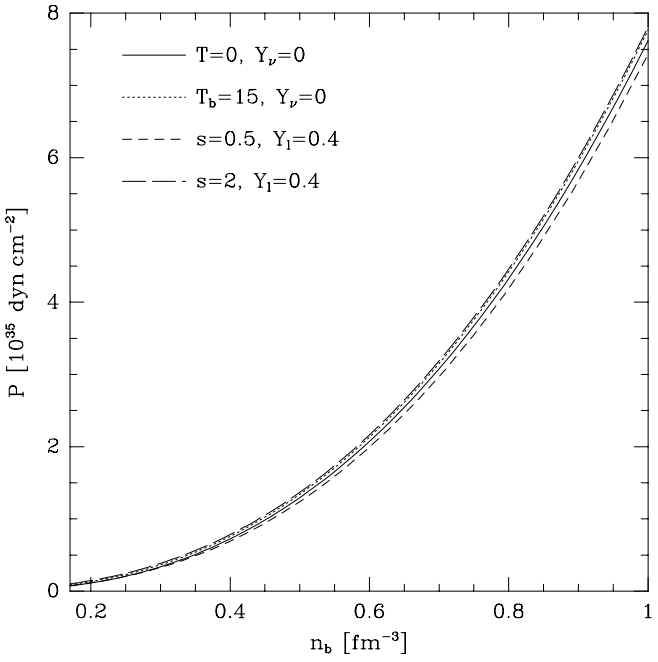

Fig. 2. Pressure versus baryon density for our model of dense hot matter, under various physical conditions, for the supranuclear densities. The curve $T = 0$ corresponds to cold catalyzed matter. The curve corresponding to $s = 0.5, Y_l = 0.4$ is unphysical, but has been added in order to visualize the importance of trapped lepton number at subnuclear densities. The low density edge of the hot, neutrino opaque core corresponds to $n_\nu = 2 \times 10^{-3}$ fm^{-3}.

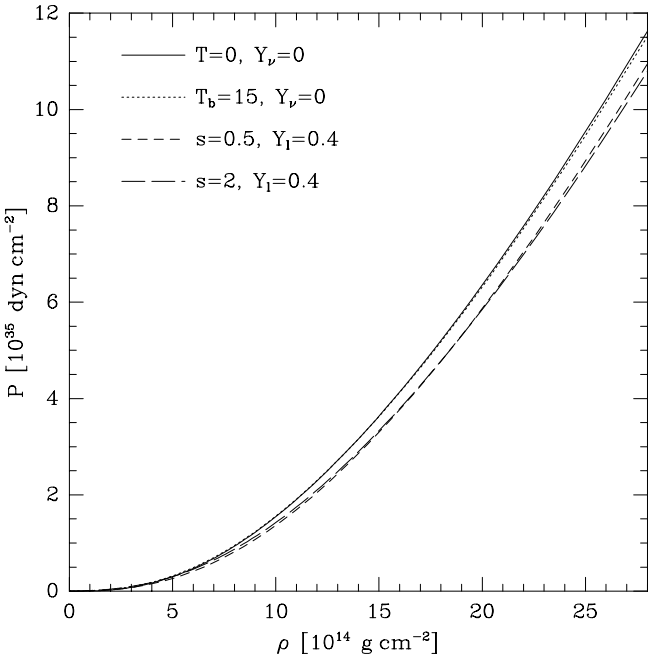

Fig. 3. Pressure versus mass–energy density for our model of dense hot matter, under various physical conditions. The curve $T = 0$ corresponds to cold catalyzed matter.

leads to a characteristic *softening* of the $P(\rho)$ EOS for large trapped lepton number, visualized in Fig. 3.

It should be stressed, that in contrast to Bombaci et al. (1995) and Prakash et al. (1997) we used a unified dense matter model, valid for both supranuclear and subnuclear densities. Also, the fact that we use various assumptions about the T and s profiles within PNS, enables us to study the relative importance of the temperature profile and that of a trapped lepton number, for the PNS models.

The mass-radius relation for the PNS models calculated using various versions of our EOS for the hot interior is shown in Fig. 4. We assumed $n_\nu = 2 \times 10^{-3}$ fm^{-3}, which was consistent with our definition of the neutrinosphere. For the sake of comparison, we also show the mass-radius relation for the $T = 0$ (cold catalyzed matter) EOS, which corresponds to cold neutron star models. In the case of an isothermal hot interior with $T_\mathrm{b} = 15$ MeV we note a very small increase of the maximum mass, as compared to the $T = 0$ case (this result is consistent with those obtained by Bombaci et al. 1995, Prakash et al. 1997, for models composed of nucleons and leptons only). However, the effect on the mass-radius relation is quite strong, and increases rapidly with decreasing stellar mass. In the case of the isentropic EOS with a trapped lepton number, $[s = 2, Y_l = 0.4]$, the softening of the high-density EOS due to the trapped Y_l leads to the decrease of M_max compared to the $T = 0$ case; as far as the value of M_max is concerned, the softening effect of Y_l prevails over that of finite s (this is consistent with results of Takatsuka 1995, Bombaci et al. 1995, and Prakash et al. 1997 for purely nucleonic models). However, the thermal effect on the stellar radius is important even in the case of $Y_l = 0.4$. This can be seen by comparing $[s = 2,\ Y_l = 0.4]$ curve with that corresponding to the unphysical, fictitious case of $[s = 0.5,\ Y_l = 0.4]$. Let us notice, that for our EOS, configurations with maximum (minimum) gravitational mass are simultaneously those with the maximum (minimum) baryon mass. The values of the minimum and maximum gravitational and baryon masses for various EOS of the PNS interiors, based on the LS-220 models of the nucleon component of dense matter, are given in Table 1. The baryon (rest) mass of a PNS model is defined by $M_\mathrm{bar} = Am_0$, where A is the total baryon number of a PNS, and m_0 is the mass of the hydrogen atom.

We find that the value of $M_\mathrm{bar,max}$ is the largest one for the $T = 0$ (cold catalyzed matter) EOS. For an isothermal hot star with $T_\mathrm{b} = 15$ MeV the total baryon mass is slightly lower than $M^{[T=0]}_\mathrm{bar,max}$, but for isentropic stars we see a significant decrease of $M_\mathrm{bar,max}$ as compared to the

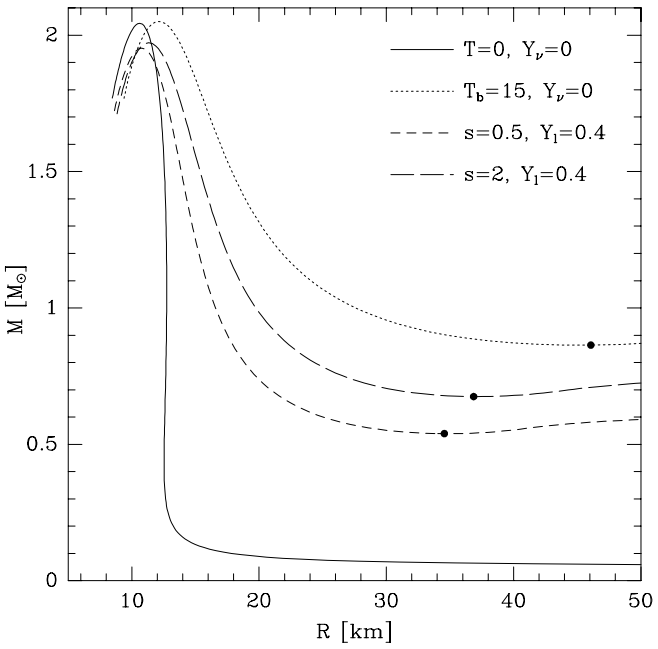

Fig. 4. The gravitational mass versus stellar radius for static models of the protoneutron stars and neutron stars, under various assumptions concerning the physical conditions within the stellar interior. The curve corresponding to $s = 0.5, Y_l = 0.4$ is unphysical, but has been added in order to visualize the relative importance of the trapped lepton number and thermal effects. The curve $T = 0$ corresponds to cold neutron stars.

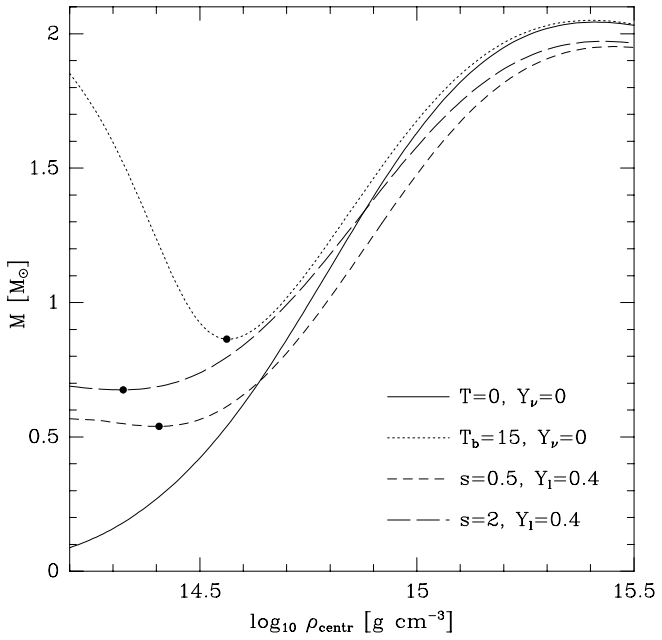

Fig. 5. The gravitational mass versus central density for static models of the protoneutron stars and neutron stars, under various assumptions concerning the physical conditions within the stellar interior. The curve corresponding to $s = 0.5, Y_l = 0.4$ is unphysical, but has been added in order to visualize the relative importance of the trapped lepton number and thermal effects. The curve $T = 0$ corresponds to cold neutron stars.

Table 1. Minimum and maximum gravitational and baryon masses of cold neutron star ($T = 0$) and isothermal ($T_\mathrm{b} = 15$ MeV, $Y_\nu = 0$) and isentropic ($s = 2, Y_l = 0.4$) protoneutron stars. Equations of state are based on the LS-220 model of the nucleon component of the matter.

EOS	M_min $[M_\odot]$	$M_\mathrm{bar,min}$ $[M_\odot]$	M_max $[M_\odot]$	$M_\mathrm{bar,max}$ $[M_\odot]$
$T = 0$, $Y_\nu = 0$	0.054	0.055	2.044	2.406
$T = 15$, $Y_\nu = 0$	0.864	0.892	2.050	2.391
$s = 2$, $Y_l = 0.4$	0.675	0.676	1.972	2.183

$T = 0$ case. A newborn hot protoneutron star with the maximum gravitational mass $M_\mathrm{max}^{[s=2,\ Y_l=0.4]} = 1.97\,M_\odot$ transforms, due to deleptonization and cooling, into a cold NS of gravitational mass of 1.9 $M_\odot$, some 0.15 $M_\odot$ less than the maximum gravitational mass of cold neutron stars (c.f. the analysis of Bombaci 1996).

For a given model of the neutrino opaque PNS core, the value of M_min depends on the location of the neutrinosphere. However, this dependence is relatively weak. For example in the case of EOS [$s = 2,\ Y_l = 0.4$] a rather drastic variation of n_ν from 2×10^{-4} fm^{-3} to 6×10^{-3} fm^{-3} implies change in $M_\mathrm{min}^{[s=2,\ Y_l=0.4]}$ from 0.686 $M_\odot$ to 0.649 $M_\odot$, respectively (the radius of these minimum–mass stars varies then from 44 km to 32.8 km, respectively).

At a given mass, the radius of a PNS is significantly larger than that of a cold NS. It should be stressed, however, that the value of radius turns out to be quite sensitive to the location of the edge of the hot neutrino-opaque interior (i.e., to the value of n_ν), especially for PNS which are not close to the M_max configuration. The choice of Prakash et al. (1997) would lead to a much smaller effect on R.

The role of the thermal and the lepton number effects are particularly pronounced in the mass - central density plots for the PNS models, Fig. 5. The low - ρ_centr segments of the $M - \rho_\mathrm{centr}$ plots for the PNS are dramatically different from that for the cold NS models. The relevance of this features for the stability of lower-mass PNS will be discussed in Sect. 7.

4. Characteristic timescales

The EOS of PNS is evolving with time, due mainly to the deleptonization process, which changes the composition of the matter, and also due to changes of the internal temperature of the star. However, these changes occur on the timescales $\tau_{\rm evol}$ ∼1-10 s (see below), which are three or more orders of magnitude longer than the dynamical timescale, governing the readjustment of pressure and gravity forces. This dynamical timescale $\tau_{\rm dyn} \sim 1$ ms corresponds also to the characteristic periods of the PNS pulsations. In view of this, we are able to decouple the PNS evolution from its dynamics, with a well defined EOS of the PNS matter.

The evolution of the PNS interior results from cooling, deleptonization, and dissipative transport processes, leading to heating. Deleptonization of PNS is due to diffusion of ν_e, driven by the gradient of their chemical potential, and occurs on a timescale $\tau_{\rm delept} \sim$ few seconds (Prakash et al. 1997). (Both $\tau_{\rm delept}$ and $\tau_{\rm cool}$ can actually be shorter, due to the presence of convection in some layers of a PNS). The PNS cooling is due to neutrino losses from the neutrinosphere; for the neutrino-opaque interior, the characteristic timescale of cooling $\tau_{\rm cool}$ is of the order of tens of seconds (Sawyer & Soni 1979). Notice, that deleptonization is accompanied by a significant heating of neutrino-opaque core. Highly degenerate ν_e diffuse out from the neutrino-opaque core, and due to $E_{\nu_e} \gg T$ they deposit most of their energy in the matter, which in view of $\tau_{\rm cool} \gg \tau_{\rm delept}$ corresponds to the net heating.

Radial pulsations of PNS are damped due to dissipative processes, resulting from the weak interactions involving nucleons and leptons. The dissipative effects can be represented in the form of a bulk viscosity of hot dense matter (Sawyer 1980). Let us consider first the case of hot interior with a significant trapped lepton number. For $Y_l = 0.3$ Sawyer (1980) gets $\tau_{\rm damp}(Y_l = 0.3) \sim 2000\,(T/10\ {\rm MeV})^2$ s. For deleptonized hot interior the characteristic timescale is somewhat shorter, $\tau_{\rm damp}(Y_\nu = 0) \sim 30\,(T/10\ {\rm MeV})^2$ s (Sawyer 1980). Still, in both cases we get $\tau_{\rm damp} \widetilde{>} 10^4 \tau_{\rm dyn}$, so that one can safely neglect damping when calculating the eigenfrequencies of radial pulsations of PNS.

Summarizing, the estimates of the evolutionary and dissipative timescales indicate, that radial pulsations of the hot interior of PNS can be treated as adiabatic, and can be studied using a well defined EOS of dense hot matter, corresponding to a given stage of evolution of a PNS.

Of course, all these remarks are valid only for the hot interior of PNS (i.e., the region below the neutrinosphere). However, the outer envelope contains less than 10^{-3} of the mass of PNS, and its influence on the eigenfrequencies of radial pulsations is negligible.

5. Linear adiabatic radial pulsations of protoneutron stars

Consider an idealized static configuration of a PNS and assume it is spherically symmetric. Using the notation of Landau & Lifshitz (1975), we write the metric for such a configuration as

$$ {\rm d}s^2 = {\rm e}^{\nu} c^2 {\rm d}t^2 - {\rm e}^{\lambda} {\rm d}r^2 - r^2({\rm d}\theta^2 + \sin^2\theta {\rm d}\phi^2)\ , \tag{7} $$

where λ and ν are functions of r.

The hydrostatic equilibrium of the static PNS is described by the Tolman-Oppenheimer-Volkoff (TOV) equations (Tolman 1939, Oppenheimer & Volkoff 1939)

$$ \frac{{\rm d}P}{{\rm d}r} = -\frac{Gm\rho}{r^2(1-\frac{2Gm}{rc^2})}\left(1+\frac{P}{\rho c^2}\right)\left(1+\frac{4\pi P r^3}{mc^2}\right)\ , \tag{8} $$

$$ \frac{{\rm d}m}{{\rm d}r} = 4\pi r^2 \rho\ , \tag{9} $$

$$ \frac{{\rm d}\nu}{{\rm d}r} = -\frac{2}{(P+\rho c^2)}\frac{{\rm d}P}{{\rm d}r}\ , \tag{10} $$

where m is the mass contained within radius r. Since our EOS of PNS can be always written in the one-parameter form $P = P(\rho)$, the TOV equations can be numerically integrated for a given central density $\rho_{\rm centr}$, yielding the stellar radius, R, and the total gravitational mass, $M = m(R)$, of the star.

The equations governing infinitesimal radial adiabatic stellar pulsations in general relativity were derived by Chandrasekhar (1964), and were rewritten by Chanmugan (1977) in a form, which turns out to be particularly suitable for numerical applications. Two important quantities, describing pulsations, are: the relative radial displacement, $\xi = \Delta r/r$, where Δr is the radial displacement of a matter element, and ΔP - the corresponding Lagrangian perturbation of the pressure. These two quantities are determined from a system of two ordinary differential equations, which we rewrite as

$$ \frac{{\rm d}\xi}{{\rm d}r} = -\frac{1}{r}\left(3\xi + \frac{\Delta P}{\Gamma P}\right) - \frac{{\rm d}P}{{\rm d}r}\frac{\xi}{(P+\rho c^2)}\ , \tag{11} $$

$$ \begin{aligned} \frac{{\rm d}\Delta P}{{\rm d}r} &= \xi\left\{\frac{\omega^2}{c^2}{\rm e}^{\lambda-\nu}\left(P+\rho c^2\right) r - 4\frac{{\rm d}P}{{\rm d}r}\right\} \\ &+ \xi\left\{\left(\frac{{\rm d}P}{{\rm d}r}\right)^2 \frac{r}{(P+\rho c^2)} - \frac{8\pi G}{c^4}{\rm e}^{\lambda}(P+\rho c^2)Pr\right\} \\ &+ \Delta P\left\{\frac{{\rm d}P}{{\rm d}r}\frac{1}{(P+\rho c^2)} - \frac{4\pi G}{c^4}(P+\rho c^2) r {\rm e}^{\lambda}\right\}\ , \end{aligned} \tag{12} $$

where Γ is a relativistic adiabatic index (see Section 6), ω is the eigenfrequency and the quantities ξ and ΔP are assumed to have a harmonic time dependence $\propto e^{i\omega t}$. Our

Eq. (12) has been obtained from a second-order pulsation equation of Chandrasekhar (1964) [his Eq. (59)], using his Eq. (35) and Eq.(36). While Eq. (11) coincides with Eq.(18) of Chanmugan (1977), our Eq. (12) - in contrast to his second equation [Eq.(19) of Chanmugan 1977] - does not show a singularity at the stellar surface. Another important advantage of our system of pulsation equations, Eq. (11, 12), stems from the fact, that they do not involve any derivatives of the adiabatic index, Γ. In view of the fact, that we used tabulated forms of the EOS and of Γ, this enabled us to reach a very high precision in solving the eigenvalue problem.

To solve equations (11) and (12) one needs two boundary conditions. The condition of regularity at $r = 0$ requires, that for $r \to 0$ the coefficient of the $1/r$-term in Eq. (11) must vanish,

$$(\Delta P)_{\rm center} = -3\,(\xi \Gamma P)_{\rm center}\ . \tag{13}$$

Our normalization of eigenfunctions corresponds to $\xi(0) = 1$. The surface of the star is determined by the condition that for $r \to R$, one has $P \to 0$. This implies

$$(\Delta P)_{\rm surface} = 0 \tag{14}$$

The problem of solving Eqs. (11), (12), can be reduced to a second order (in ξ), linear radial wave equation, of the Sturm-Liouville type. The quantity ω^2 is the eigenvalue of the Sturm-Liouville problem with boundary conditions given by Eqs. (13), (14). For a given static model of a PNS, we get a set of the eigenvalues $\omega_0^2 < \omega_1^2 < ... < \omega_{\rm n}^2 < ...$, with corresponding eigenfunctions $\xi_0, \xi_1, ..., \xi_{\rm n}, ...$, where the eigenfunction $\xi_{\rm n}$ has n nodes within the star, $0 \le r \le R$ (see, e.g., Cox 1980).

A given static model is stable with respect to small, radial, adiabatic perturbations (pulsations), if $\omega_{\rm n}^2 > 0$ for all n. The configuration is marginally stable, if the lowest eigenfrequency $\omega_0 = 0$.

6. Adiabatic indices

The adiabatic index within the star, Γ, plays a central role for both the linear radial oscillations, and for the stability of PNS. In what follows, we will restrict ourselves to the case of the neutrino-opaque interior; the layer above the neutrinosphere contains only about 10^{-3} of the total mass, and does not influence neither the spectrum of radial oscillations, nor the stability of PNS.

Under physical conditions prevailing within the hot interior of a PNS, the perturbation of a local nucleon density, δn, of a matter element during radial oscillations, takes place at constant entropy per baryon, s, and constant electron lepton number per baryon, Y_l. Due to high density and temperature, all constituents of matter can be considered as being in thermodynamic equilibrium (the timescale of reactions leading to thermodynamic equilibrium, $\tau_{\rm react}$, is much shorter, then the pulsation timescale, $\tau_{\rm puls} \sim \tau_{\rm dyn}$). The adiabatic index, governing linear perturbation of the pressure within the star under these conditions, will be denoted by $\Gamma_{\rm a}$. It will be given by

$$\Gamma_{\rm a} \equiv \frac{n}{P}\left(\frac{{\rm d}P}{{\rm d}n}\right)_{s,Y_l}\ , \tag{15}$$

where the derivative is to be calculated at fixed s and Y_l. It should be stressed, that the calculation of $\Gamma_{\rm a}$ requires more than just the knowledge of the EOS of the PNS interior. Namely, one needs to know the perturbed EOS, under the constraint of constant s and Y_l, and assuming the thermodynamic equilibrium of matter constituents.

In the case of dense matter one can define several Γ's, which are physically (and numerically) different from $\Gamma_{\rm a}$. The EOS of dense hot matter within a static PNS yields the quantity

$$\Gamma_{\rm EOS} \equiv \frac{n}{P}\left(\frac{{\rm d}P}{{\rm d}n}\right)_{\rm star}\ . \tag{16}$$

Strictly speaking $\Gamma_{\rm EOS}$ is not an "adiabatic" index unless the entropy s is constant throughout a star.

In the case of a sufficiently cold matter, the reactions between matter constituents are so slow, that the matter composition remains fixed (frozen) during perturbations, because $\tau_{\rm react} \gg \tau_{\rm dyn}$. Also, neutrinos do not contribute then to the thermodynamic quantities of the matter. In such a case, the appropriate adiabatic index would read

$$\Gamma_{\rm frozen} \equiv \frac{n}{P}\left(\frac{{\rm d}P}{{\rm d}n}\right)_{s,Y_e}\ , \tag{17}$$

where s, Y_e correspond to the equilibrium model. The quantity $\Gamma_{\rm frozen}$ is relevant for radial pulsations of standard, cold neutron stars, where the difference between $\Gamma_{\rm frozen}$ and $\Gamma_{\rm EOS}$ has interesting consequences for the stability of the cold NS models in the vicinity of $M_{\rm max}$ (Gourgoulhon et al. 1995).

The dependence of various Γ's on the matter density in the PNS interior, for two models of the hot neutrino-opaque core of PNS, is displayed in Fig. 5, 6. Above nuclear density (i.e., for bulk, homogeneous matter) $\Gamma_{\rm frozen}$ is the highest of all Γ's; freezing of lepton composition stiffens the matter (c.f. §81 of Landau & Lifshitz (1987)). In the case of the isothermal core, Fig. 6, $\Gamma_{\rm EOS}$ is significantly lower than $\Gamma_{\rm a}$ and $\Gamma_{\rm frozen}$, for subnuclear densities above n_ν (this results from the fact of a significant density dependence of the entropy per baryon, in this density interval). For isothermal models $\Gamma_{\rm EOS} \equiv \Gamma_{\rm star} < \Gamma_{\rm a}$, except for the region close to and below the neutrinosphere: for $\rho > 10^{13}$ g cm^{-3} our isothermal PNS models are convectively stable. The differences between various Γ's differences are much smaller in the case of the isentropic core, where fixing s throughout the star and within the EOS makes $\Gamma_{\rm EOS}$ and $\Gamma_{\rm a}$ undistinguishable, except near the neutrinosphere, where a dramatic drop in s and in T produces a strong deviation of $\Gamma_{\rm EOS}$ from both $\Gamma_{\rm a}$ and $\Gamma_{\rm frozen}$.

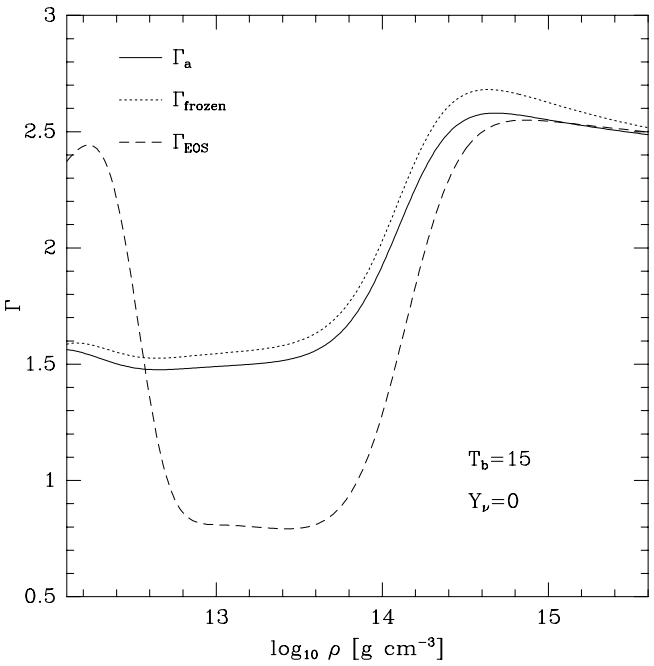

Fig. 6. Parameters $\Gamma_{\rm a}$, $\Gamma_{\rm EOS}$, and $\Gamma_{\rm frozen}$, versus matter density, for the isothermal hot interior with $T_{\rm b} = 15$ MeV and with no trapped lepton number. The outer edge of the hot core has been located at $\rho_\nu = 3.5 \times 10^{12}$ g cm^{-3}, and the rapid changes in the Γ's below n_ν results from the temperature drop in the neutrinosphere of the PNS.

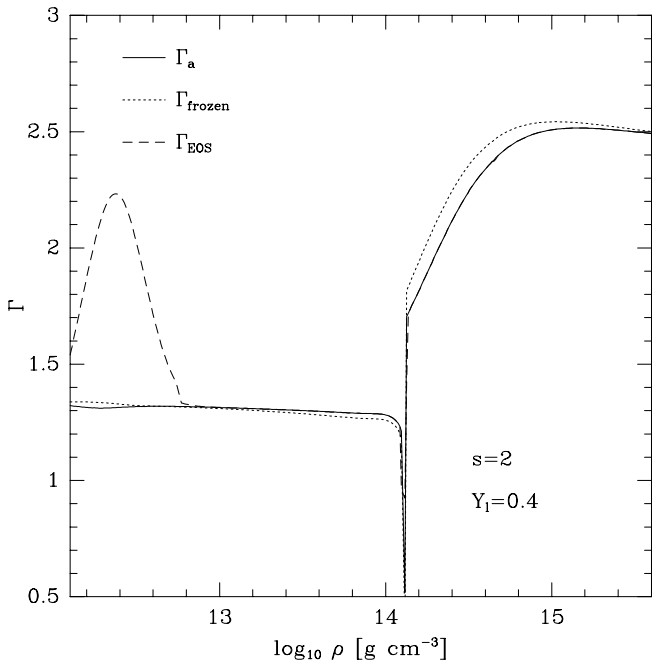

Fig. 7. Parameters $\Gamma_{\rm a}$, $\Gamma_{\rm EOS}$, and $\Gamma_{\rm frozen}$, versus matter density, for the isentropic hot interior with $s = 2$ and with trapped lepton fraction $Y_l = 0.4$. The outer edge of the hot core has been located at $\rho_\nu = 3.5 \times 10^{12}$ g cm^{-3}, and the rapid changes in the Γ's below n_ν results from the temperature drop in the neutrinosphere of the PNS. The very steep drop in Γ's above 10^{14} g cm^{-3} results from the phase transition from matter with nuclei to bulk (homogeneous) dense matter.

The differences between $\Gamma_{\rm frozen}$ and $\Gamma_{\rm a}$ are mainly due to the changes of Y_e throughout the star. The quantity $\Gamma_{\rm frozen}$ corresponds to adiabatic pulsations keeping Y_e fixed, while $\Gamma_{\rm a}$ was calculated assuming beta equilibrium during adiabatic oscillations at fixed Y_l. It should be stressed, that pulsational properties of PNS are determined essentially by the values of the relevant Γ well above the density n_ν. The outer layer with $n < n_\nu$ contains a very small fraction of stellar mass, and therefore rapid variations of Γ close to n_ν have no effect on the global dynamics of PNS.

7. Eigenfrequencies and instabilities

The effects of high temperature and those of the trapped neutrinos influence both the EOS and the adiabatic index of the interior of PNS. Our calculations show a rather strong influence of these effects on the eigenfunctions and the eigenfrequencies of radial pulsations of PNS. Also, these effects imply significant differences, especially within some (observationally interesting) interval of stellar masses, between pulsational properties of PNS and cold NS.

In Fig. 8 we plotted the eigenfrequency of the fundamental mode of the PNS pulsations, versus stellar mass, for several models of the EOS of the hot interior. For the sake of comparison, we have presented also the corresponding plot for cold neutron stars. The effect of finite entropy and of trapped lepton number on ω_0 depends rather strongly on the stellar mass. The relativistic instability takes place very close to $M_{\rm max}$, so that the "classical stability criterion" (protoneutron star models to the left of the maximum in the $M - R$ plot, Fig. 4, are secularly unstable with respect to the $n = 0$ oscillations) is valid to a very good approximation. Generally, entropy and trapped lepton number soften the $n = 0$ mode with respect to the $T = 0$ models. This softening is particularly strong for lower stellar mass. In the case of $s = 2$, $Y_l = 0.4$ PNS, the fundamental mode becomes secularly unstable at $M = 0.676\ M_\odot$, very close to the minimum of the $M-R$ curve, Fig. 4. The classical stability criterion gives therefore a rather precise location of the instability point for the *isentropic* PNS: the models to the right of the minimum in the $M - R$ curve are unstable with respect to the radial pulsations in the fundamental mode. However, the value of $M_{\rm min}$ is dramatically larger than that for the *cold* ($T = 0$) neutron stars. We have $M_{\rm min}[s = 2, Y_l = 0.4] = 0.675\ M_\odot$, while $M_{\rm min}[T = 0] = 0.054\ M_\odot$.

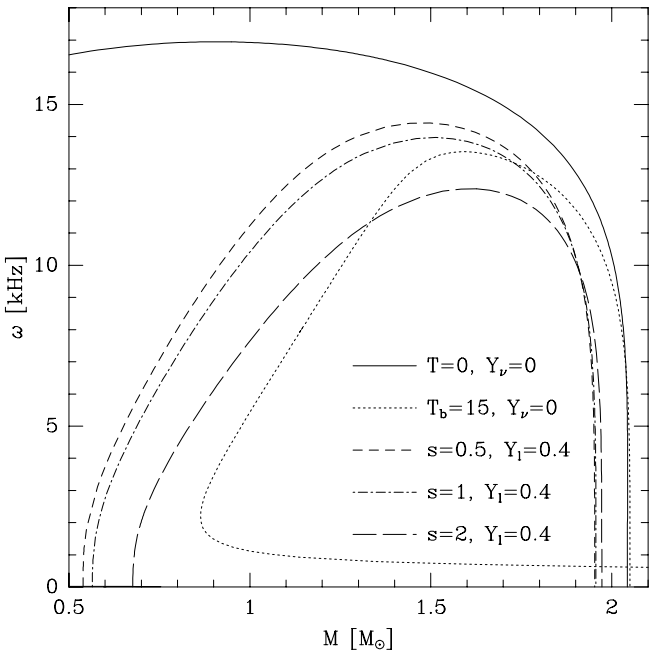

Fig. 8. The eigenfrequencies of the fundamental mode, $n = 0$, versus stellar mass for considered models of dense matter. The nearly horizontal part of the curve for $T_{\rm b} = 15$ MeV model corresponds to the configurations with central density below the value corresponding to the minimum mass of PNS. For the sake of comparison we also show corresponding curve for cold neutron stars.

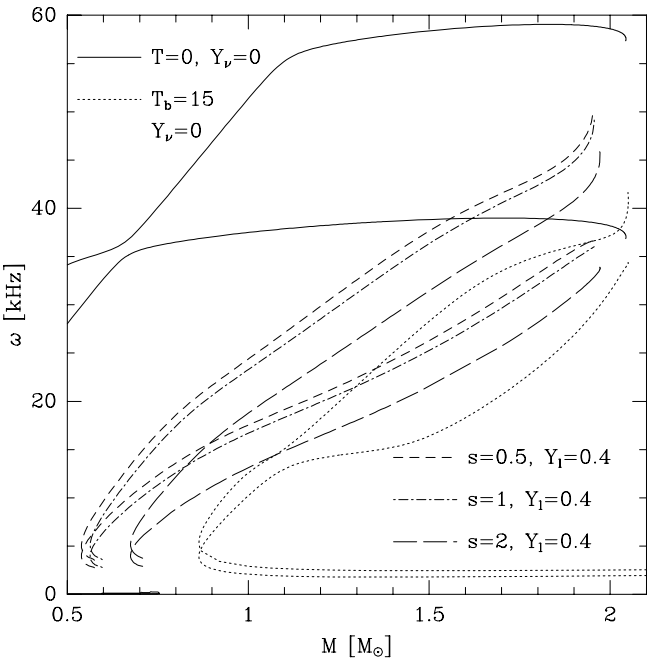

Fig. 9. The eigenfrequencies of the first and second overtone, $n = 1, 2$, versus stellar mass for considered models of dense matter. For the sake of comparison we also show corresponding curves for cold neutron stars.

In Fig. 9 we plotted the eigenfrequencies of the $n = 1$, 2 radial modes versus stellar mass, for the isentropic models of the hot PNS cores. For the sake of comparison, we have shown also the corresponding plots for cold NS. The differences between the NS and the PNS $n = 1$, 2 eigenfrequencies are very large, except for a narrow interval of masses in the vicity of the maximum mass. These differences reflect the drastic differences in the structure of the outer layers of the PNS and the NS models. Generally, PNS are much softer with respect to the $n = 1$, 2 radial modes. Different structure of the outer layers of stellar models with isentropic and isothermal cores, implies strong differences in the spectra of the lowest three modes of radial pulsations. Clearly, the $M < 1\ M_{\odot}$ isothermal models are much "softer" with respects to all considered modes of radial pulsations, than the isentropic ones; this is due to the fact that they are significantly less compact (inflated by the thermal effects) than their isentropic counterparts. The characteristic "turning points" and the intermodal intersections for the PNS models on the low-mass side of Fig. 9, are due to the existence of minimum masses. However, it should be stressed that the frequency intersection points, seen in the case of the case of the $n = 1$ and the $n = 2$ eigenfrequencies, do not correspond to the same configuration of the PNS (while having the same mass, these configurations have different central densities, see Figures 10, 11).

The situation is less complicated in the case of the plots of the eigenfrequencies versus the central density of the stellar models, $\rho_{\rm centr}$, presented in Figures 10 and 11. At lower central densities the values of $\omega_{\rm n}$ decrease monotonically, but very slowly, with decreasing central density.

The effects of temperature and of the differences in adiabatic indices Γ are particularly strong in the case of the isothermal hot interior, with $T = T_{\infty}(g_{00})^{-1/2}$. Our results for the first three radial modes ($n = 0$, 1, 2), for $T_{\rm b} = 15$ MeV, are given in Fig. 11, where we show also for comparison results obtained for cold NS. Three curves presented in Fig. 11 correspond to three different choices of Γ, governing the changes of pressure vs. density during pulsations. Although only results for $\Gamma = \Gamma_{\rm a}$ are physical, the difference between curves visualizes the role of the proper treatment of chemical equilibrium and adiabacity when the PNS star is oscillating. $\Gamma_{\rm EOS}$ is determined by the equation of state of the matter within a *static* model of PNS. As one can see from Fig. 11, the use of $\Gamma_{\rm EOS}$ leads usually to a significant underestimating of the eigenfrequencies of oscillation modes. A notable exception from this behavior is that of the fundamental mode near the maximum mass of PNS, for which results obtained using $\Gamma_{\rm EOS}$ are very close to those obtained using $\Gamma_{\rm a}$. Con-

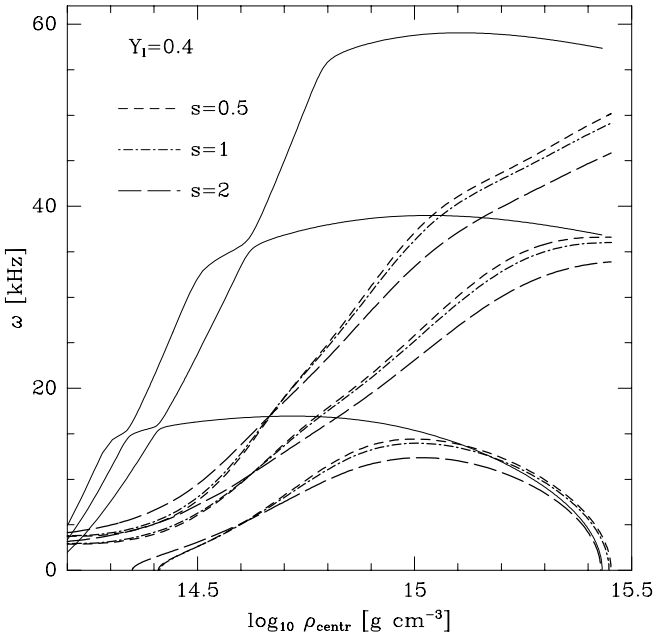

Fig. 10. The eigenfrequencies of three lowest radial modes, $n = 0,\ 1,\ 2$, for hot isentropic protoneutron stars with trapped lepton fraction $Y_l = 0.4$, versus central density. For the sake of comparison we also show corresponding curves for cold neutron stars (thin solid lines).

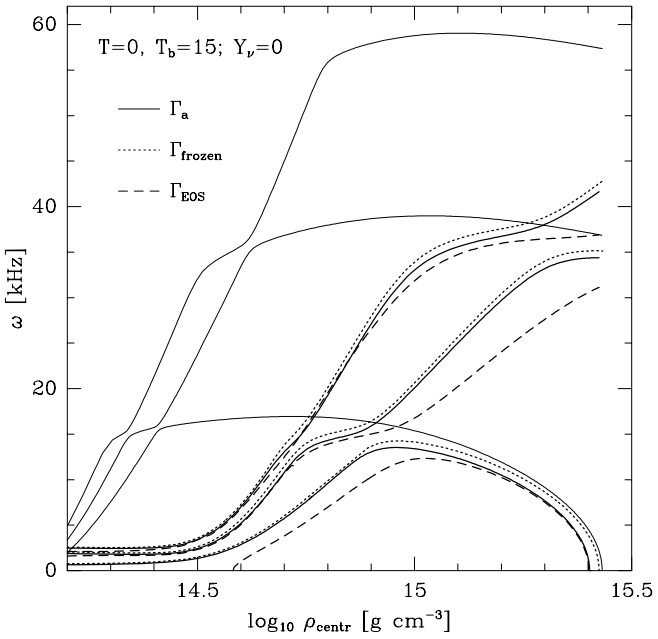

Fig. 11. The eigenfrequencies of three lowest radial modes, , $n = 0,\ 1,\ 2$, for protoneutron stars with hot isothermal core with $T_{\rm b} = 15$ MeV, versus central density For the sake of comparison we also show corresponding curves for cold neutron stars (thin solid lines).

sequently, the classical static stability criterion at $M_{\rm max}$ works rather well also for the *isothermal* PNS.

However, the difference between $\omega_0^{\rm (EOS)}$ and actual ω_0 increases with decreasing $\rho_{\rm centr}$ and the static stability criterion at $M_{\rm min}$ does not hold. We have $M_{\rm min}[T_{\rm b} = 15\ {\rm MeV}] = 0.86\ M_\odot$ but configurations in the neighbourhood of the mass minimum turn out to be stable with respect to the fundamental mode of the radial pulsations, calculated using the *actual* (physical) values of $\Gamma = \Gamma_{\rm a}$.

In Fig. 11 we can see an interesting phenomenon — abrupt, nearly stepwise changes in frequencies of the consecutive (neighbouring) oscillation modes, especially pronounced for cold neutron stars, but clearly visible also in the case of $T_{\rm b} = 15$ MeV, $Y_\nu = 0$ models of PNS. This is the "avoided crossing" phenomenon of the *radial* modes of neutron stars. This effect is known from the analysis of the *nonradial* oscillations in "ordinary" stars (Aizenman, Smeyers and Weigert (1977), Christensen–Dalsgaard (1980)) and has been recently considered by Lee and Strohmayer (1996) for *nonradial* oscillations of rotating neutron stars. Our preliminary studies of this effect indicate, that the stepwise changes of ω_n are due to the change of the character of the standing-wave solution for the eigenproblem. Namely, at the "avoided crossing' point the solution changes from the standing wave localized mainly in the outer layer of the star, to that localized predominantly in the central core. This topic will be discussed in separate paper (Gondek et al. 1996).

8. Discussion and conclusions

The birth of protoneutron stars is a dynamical process, and a newborn protoneutron star is expected to pulsate. These pulsations were excited during star formation. In the present paper we studied linear, radial pulsations of protoneutron stars, under various assumptions concerning hot stellar core, and for a large interval of stellar masses.

The spectrum of the lowest modes of radial pulsations of protoneutron stars is quite different from that of cold neutron stars. Generally, protoneutron stars are significantly softer with respect to the radial pulsations, than cold neutron stars, and this difference increases for higher modes and for lower stellar masses. These differences stem from different structure of protoneutron stars, which in contrast to cold neutron stars have extended envelopes, inflated by thermal and trapped neutrinos effects.

The standard static criteria of stability of neutron star models were derived under the assumption of cold, catalyzed matter (Harrison et al. 1965). We have shown, that to a rather good approximation, the configuration with maximum mass separates stable configurations from the secularly unstable ones (with respect to fundamental mode of small radial pulsations). Therefore, despite thermal and neutrino trapping effects, one can apply standard "maximum mass" criterion to locate the relativistic insta-

bility of protoneutron stars, both for the isentropic and the isothermal hot, neutrino opaque cores.

The role of thermal effects increases with decreasing stellar mass. Static "minimum mass" criterion does apply with a rather good precision to protoneutron stars with hot isentropic, neutrino opaque cores. This is due to the fact, that the perturbation itself conserves entropy (pulsations are adiabatic), and equilibration of matter is sufficiently fast. However, the "minimum mass" criterion does not apply to protoneutron stars with hot isothermal cores. In both cases, the minimum masses of protoneutron stars are rather large (for our models of dense hot matter we obtained the values of 0.675 $M_\odot$ and 0.86 $M_\odot$ for the isentropic ($s = 2$, $Y_l = 0.4$) and the isothermal ($T_\mathrm{b} = 15$ MeV) models, respectively.

Our treatment of the thermal state of the protoneutron star interior should be considered as very crude. The temperature profile might be affected by convection. Also, our method of locating the neutrinosphere was very approximate. Clearly, the treatment of thermal effects can be refined, but we do not think this will significantly change our main results.

Our calculations were performed for only one model of the nucleon component of dense hot matter. The model was realistic, and enabled us to treat in a unified way the whole interior (core as well as the envelope) of the protoneutron star. However, in view of the uncertainties in the EOS of dense matter at supranuclear densities, one should of course study the whole range of theoretical possibilities, for a broad set - from soft to stiff - of supranuclear, high temperature EOS. An example of such an investigation in the case of the *static* protoneutron stars, is the study of Prakash et al. (1997).

In a hypothetical scenario, proposed by Brown and Bethe (1994), a protoneutron star borns as a hot, lepton rich object, composed of nucleons and leptons. If the final state of cold neutron star is characterized by a large electron fraction, due to the appearance of a large amplitude K^- - condensate (or because a large fraction of baryons are negatively charged hyperons), then the cold equation of state of neutron star matter is softer than that of hot, lepton rich protoneutron star. In such a case, $M_{\mathrm{bar,max}}(\mathrm{NS}) < M_{\mathrm{bar,max}}(\mathrm{PNS})$, and all protoneutron stars with baryon mass exceeding $M_{\mathrm{bar,max}}(\mathrm{NS})$ will eventually collapse into black holes. Clearly, in such a case the problem of stability of the protoneutron star models in the vicinity of $M_{\mathrm{bar,max}}(\mathrm{PNS})$ with respect to radial pulsations looses its significance.

Acknowledgements. We are very grateful to W. Dziembowski for introducing us into the topic of the "avoided crossing" phenomena, for his numerous helpful remarks, and for careful reading of the manuscript. This research was partially supported by the KBN grant No. P304 014 07 and by the KBN grant No. 2P03D01211 for D. Gondek. D. Gondek and P. Haensel were also supported by the program Réseau Formation Recherche of the French Ministère de l'Enseignement Supérieure et de la Recherche.

References

Aizenman M.L., Smeyers P., Weigert A., 1977 A&A, 58, 41
Baumgarte T.W., S.L. Shapiro, S.A. Teukolsky, 1996, ApJ 458, 680
Bombaci I., Prakash M., Prakash M., Ellis P.J., Lattimer J.M., Brown G.E., 1995, Nucl. Phys. A, 583, 623
Bombaci I., 1996, A&A 305, 871
Brown G.E., Bethe H.A., 1994, ApJ 423, 659
Burrows A., Lattimer J.M., 1986, ApJ, 307, 178
Chandrasekhar S., 1964, ApJ 140, 417
Chanmugan G., 1977, ApJ 217, 799
Christensen–Dalsgaard J., 1980, MNRAS, 190, 765
Cox J.P., 1980, "Theory of stellar pulsations", Princeton University Press, Princeton
Gourgoulhon E., Haensel P., Gondek D., 1995, A&A, 294, 747
Harrison B.K, Thorne K.S., Wakano M., Wheeler J.A., 1965, "Gravitation Theory and Gravitational Collapse", University of Chicago Press, Chicago
Landau L.D., Lifshitz E.M., 1975, "Classical theory of fields", Pergamon Press, Oxford
Landau L.D., Lifshitz E.M., 1987, "Fluid Mechanics", Pergamon Press, Oxford
Lattimer J.M., Swesty F.D., 1991, Nucl. Phys. A535, 331
Lee U., Strohmayer T.E., 1996, A&A 311, 155
Oppenheimer J.R., Volkoff G.M., 1939, Phys. Rev. 55, 374
Pandharipande V.R., Pethick C.J., Thorsson V., 1995, Phys.Rev.Lett. 75, 4567
Prakash M., Bombaci I., Prakash M., Ellis P.J., Lattimer J.M., Knorren R., 1997, Phys. Reports, in press
Sawyer R.F., 1980, ApJ 237, 187
Sawyer R.F., Soni A., 1979, ApJ 230, 859
Takatsuka T., 1995, Nucl. Phys. A588, 365c
Tolman R.C., 1939, Phys. Rev. 55, 364
Zeldovich Ya.B., Novikov I.D., 1971, "Relativistic astrophysics", vol. I, University of Chicago Press, Chicago

This article was processed by the author using Springer-Verlag LaTeX A&A style file *L-AA* version 3.